

This material has been copied under licence from CANCOPY. Resale or further copying of this material is strictly prohibited.

Le présent document a été reproduit avec l'autorisation de CANCOPY. La revente ou la reproduction ultérieure en sont strictement interdites.

Thermal-Neutron Behavior in Cluster-Type Plutonium Fuel Lattices

T. Wakabayashi and Y. Hachiya

Power Reactor and Nuclear Fuel Development Corporation, Oarai Engineering Center
4002 Oarai-machi, Ibaraki-ken, Japan

Received November 19, 1976

Revised February 14, 1977

The thermal-neutron behavior in a highly heterogeneous cluster-type plutonium fuel lattice has been studied through the measurements of the dysprosium reaction-rate distribution in a unit cell covering three plutonium fuel elements, four coolant voids, and two lattice pitches. The study included comparison with the results obtained with UO_2 fuel.

A new technique for locating the foils has been developed, resulting in an accurate measurement of the thermal-neutron flux distribution.

Depression of the thermal-neutron flux in the fuel region is larger in the plutonium fuel lattice than in the uranium lattice because thermal-neutron absorption in the plutonium fuel is enhanced by the resonances of ^{239}Pu and ^{241}Pu at 0.3 eV. In addition, the $1/v$ cross section of plutonium is larger than that of uranium. This property of the plutonium fuel appears markedly at 100% void fraction, but less at 0% because this property is weakened by the presence of H_2O coolant.

The results of calculations obtained by means of the LAMP-DCA code showed good agreement with experimentally determined data within 5%.

I. INTRODUCTION

In a plutonium fuel lattice, the behavior of neutrons, especially of thermal neutrons, is inherently more complicated than that in uranium fuel lattices, because isotopes of plutonium have large neutron resonances in the low-energy region, making the physics characteristics of plutonium fuel lattices more difficult to calculate than those of uranium lattices.

This situation becomes very serious when the plutonium fuel is utilized in the cluster-type fuel lattices such as the lattice of FUGEN (Refs. 1 and 2), which is a heavy-water-moderated, light-water-cooled thermal reactor because, due to its high heterogeneity, fine thermal-neutron flux distributions are largely affected by slight changes in fuel enrichment, in plutonium isotopic composition, and in the volume ratio between fuel and

coolant and between fuel and moderator. Accordingly, accurate measurement of the thermal-neutron flux distribution, as affected by slight changes in the lattice condition, is indispensable for clarification of the thermal-neutron behavior and for the evaluation and improvement of calculational accuracy.

The experimental studies, which have the same or better measurement accuracy than those of uranium fuel,³⁻⁷ are relatively insufficient for the cluster-type plutonium fuel lattices.^{3,8-10}

¹Y. HACHIYA and H. HATAKENAKA, *J. Nucl. Sci. Technol.*, **9**, 629 (1972).

²K. YAMAMOTO, K. KURIHARA, M. MATSUOKA, and T. WAJIMA, *J. Nucl. Sci. Technol.*, **9**, 705 (1972).

³H. SAKATA, Y. HACHIYA, K. SHIBA, N. FUKUMURA, and A. NISHI, *Trans. Am. Nucl. Soc.*, **16**, 267 (1973).

⁴Y. HACHIYA, N. FUKUMURA, A. NISHI, K. IJIMA, and H. SAKATA, *J. Nucl. Sci. Technol.*, **13**, 618 (1976).

⁵C. G. CAMPBELL and I. JOHNSTONE, *J. Brit. Nucl. Energy Soc.*, **5**, 168 (1966).

⁶L. C. SCHMID, B. R. LEONARD, Jr., R. C. LIKALA, and R. I. SMITH, "Reactor Physics Data for the Utilization of Plutonium in Thermal Power Reactors," BNWL-801, Pacific Northwest Laboratories (1968).

⁷V. O. UOTINEN, B. R. LEONARD, Jr., and R. C. LIKALA, *Nucl. Technol.*, **18**, 115 (1973).

¹⁰T. WAKABAYASHI and Y. HACHIYA, *Trans. Am. Nucl. Soc.*, **21**, 466 (1975).

¹S. SHIMA and S. SAWAI, "The Fugen Project," CNA 13th Annual Int. Conf., Toronto, CNA 73-204, Canadian Nuclear Association (1973).

²T. TAKEKOSHI and S. SAWAI, "Use of Plutonium in Heavy Water Moderated Boiling Light Water Cooled Reactor," N 341 72-16, Power Reactor and Nuclear Fuel Development Corporation (1972).

The
is to m
plutoni
dyspro
cell foll
fraction
position
cation
compare
previous
The
compare
METHU
FUGEN
(b) with
veloped
lational

A cl
consists
cladding
cluster
counting
8 pins
layer.
loaded
fuel, coi
into a
were su
the upper
the clus
fuel me
The
aluminu
sure tu
This pa
lattice
cylindri
plates a
3005 mi
was ma

¹¹R. J
Programm
or STRE
Authority
¹²M. J
LAH II-
Physics A
480, U.K.
¹³K. J
Code," Pr
Society of
¹⁴K. I
TANI, ("I
DCA) for
Meeting
(1974).

The main objective of the present experiment is to make the thermal-neutron behavior in the plutonium-fueled lattice clear by measuring the dysprosium reaction rate distribution in a unit cell following systematic changes in coolant void fraction, fuel enrichment, plutonium isotopic composition, and the lattice pitch. For better clarification of the behavior, the results are also compared with those of UO_2 fuel obtained in the previous experiment.⁶

The experimental results are systematically compared with (a) those calculated with the METHUSELAH-II code,^{11,12} on which much of the FUGEN core design calculations are based, and (b) with the LAMP-DCA code,^{13,14} which is developed for the purpose of obtaining better calculational accuracy.

II. EXPERIMENTAL FACILITY

A cluster used for the present experiments consists of 28 PuO_2 - UO_2 fuel pins with Zircaloy-2 cladding as shown in Fig. 1. The fuel pins in the cluster were arranged in three concentric layers; counting from center there are 4 pins in the first, 8 pins in the second, and 16 pins in the third layer. Inconel-X springs under compression and loaded at the upper end of the element hold the fuel compacted. These fuel pins were arranged into a 28-pin cluster by aluminum spacers that were supported by aluminum hanger wires between the upper and lower tie plates. The total length of the cluster was 2223 mm, including the standard fuel meat length of 2000 mm.

The cluster was located in a double-walled aluminum tube; the inner one is called the pressure tube and the outer one the calandria tube. This pair of tubes was positioned in a square lattice having a 22.5- or 25.0-cm pitch in a cylindrical core tank by upper and lower grid plates also made of aluminum. The core tank was 3005 mm in diameter and 3500 mm in height, and was made of 10-mm-thick aluminum. Heavy water

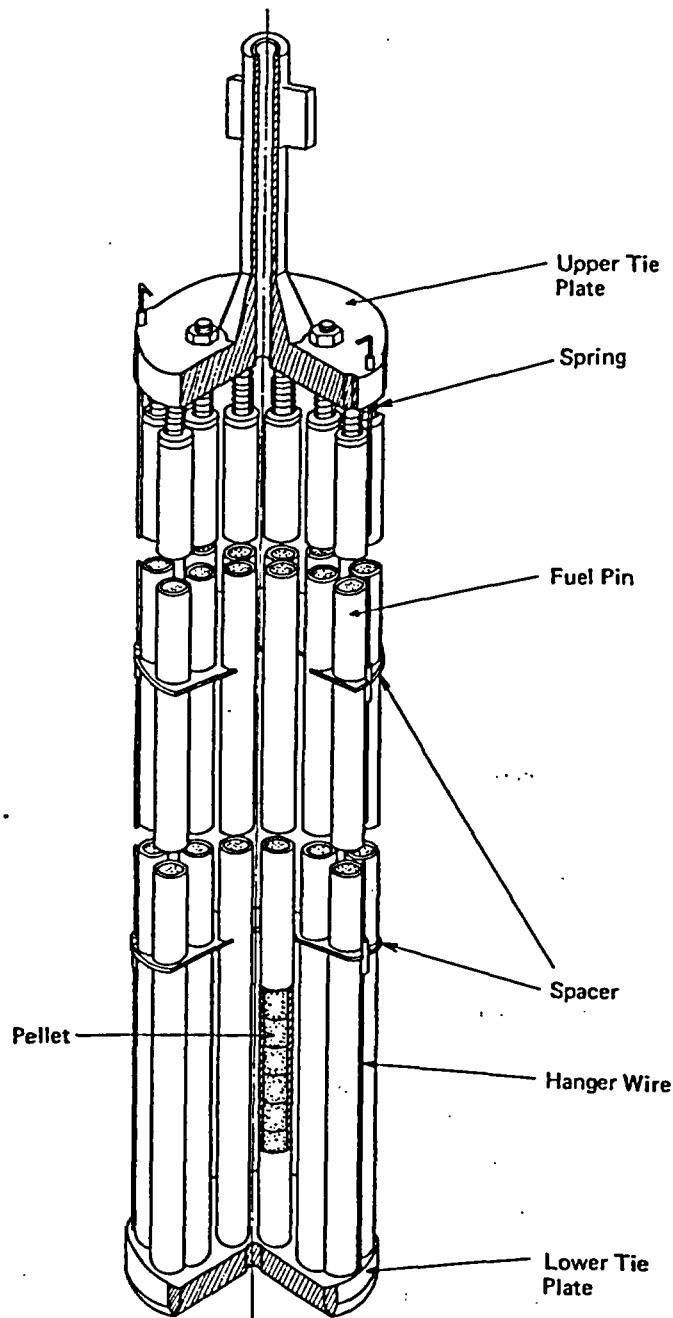


Fig. 1. Schematic drawing of a fuel cluster.

¹¹R. ALPIAR, "METHUSELAH I-A Universal Assessment Programme for Liquid Moderated Reactor Cells, Using IBM 7090 or STRETCH Computers," AEEW-R135, U.K. Atomic Energy Authority, Winfrith (1964).

¹²M. J. BRINKWORTH and J. A. GRIFFITHS, "METHUSELAH II-A Fortran Program and Nuclear Data Library for the Physics Assessment of Liquid-Moderated Reactors," AEEW-R 480, U.K. Atomic Energy Authority (1966).

¹³K. TSUCHIHASHI, "Analysis of SG3 Lattice by LAMP-A Code," Preprint F16, 1971 Annual Meeting of the Atomic Energy Society of Japan (in Japanese) (1971).

¹⁴K. IJIMA, Y. HACHIYA, H. SAKATA, and H. KADOTANI, "Improvements of Detailed Calculation Code (LAMP-DCA) for Cluster-Type Fuel Lattice," Preprint A6, 1974 Fall Meeting of the Atomic Energy Society of Japan (in Japanese) (1974).

of 99.5 mol% purity was the moderator. The dimensions and compositions of the present experimental lattices are listed in Table I.

The quantity and composition of coolant in the pressure tubes of the cluster were varied to simulate a range of effective void fractions from 0% (when filled with light water) to 100% (when filled with air). Two intermediate void fractions, 30 and 70%, were simulated by the D_2O - H_2O - H_3BO_3 ,

TABLE I

Lattice Dimensions and Compositions

Cluster	
Radius of each layer	
1st	13.13 mm
2nd	30.00 mm
3rd	47.58 mm
Hanger wire	
Diameter	2.0 mm
Material	Al
Spacer	
Diameter	114.4 mm
Material	Al
Cluster length	2223 mm
Standard fuel meat length	2000 mm
Pressure tube	
o.d.	121.0 mm
i.d.	116.8 mm
Material	Al
Calandria tube	
o.d.	136.5 mm
i.d.	132.5 mm
Material	Al
Moderator	
Material	D ₂ O
Purity	99.5 mol%
Core tank	
o.d.	3025 mm
i.d.	3005 mm
Height	3500 mm
Material	Al
Lattice pitch	22.5 or 25.0 cm (square lattice)
Upper and lower grid plate	
Material	Al
Temperature	20°C

mixtures specified in Table II. The mixtures of light and heavy water simulated slowing down effects of voids, and small amounts of boric acid accurately simulated the effective absorption. In each experiment, the coolant level was kept as close as possible to that of the D₂O moderator.

Three different mixtures of plutonium oxide in natural uranium oxide were available for the present experiment. The plutonium fuel enrichment is defined as the weight percent of PuO₂ in the PuO₂-UO₂ mixture. Two fuels, of 0.54 and 0.87% enrichment, were made of standard-grade plutonium (~91% fissile plutonium) and of reactor-grade plutonium (~74% fissile plutonium), respectively. The specifications for each fuel are listed in Table III.

TABLE II

Composition of Experimental Coolant Mixture

Material (wt%)	Coolant Void Fraction (%)			
	0	30	70	100
H ₂ O	100	63.17	18.07	0
D ₂ O	0	36.82	81.91	0
H ₃ BO ₃	0	0.0092	0.0215	0

These PuO₂-UO₂ fuel clusters were arranged in the central part of the core, as shown in Fig. 2, in a square 5 × 5 lattice with one exception, and the surrounding part was loaded with 1.2-wt%-enriched UO₂ fuel clusters having the same dimensions as those of the PuO₂-UO₂ fuel. In the case of the standard-grade 0.87-wt% PuO₂-UO₂ fuel with a coolant void fraction of 0% on the 22.5-cm pitch, nine clusters were arranged 3 × 3 in the central part so as not to make the D₂O critical level too low. As a result, the experimental D₂O levels, the heights from the bottom end of the fuel meat to the D₂O surface, ranged from 83.0 to 104.0 cm. A previous experiment³ showed that an equilibrium of the neutron energy spectrum in the central unit cell was satisfactorily attained in at least nine clusters.

III. MEASUREMENT

The dysprosium reaction rate distributions in the unit cell were measured by a 0.1-mm-thick dysprosium-aluminum alloy (4.0 wt% dysprosium) foils in the central unit cell as shown in Fig. 3. Measurement positions of the foils in the unit cell are shown in Fig. 3. They are within the plutonium fuel pins, in the coolant, on both the inside and the outside surfaces of the pressure tube and the calandria tube, and in the D₂O moderator.

For measurements within the plutonium fuel pins, four 14.8-mm-diam foils were set in positions F-1, F-2, F-3, and F-3', shown in Fig. 3. The foil arrangement within the plutonium fuel pin is shown in Fig. 4.

The dysprosium foils were covered with 0.02-mm-thick aluminum foils as a cassette to protect them from contamination by PuO₂-UO₂ powder and fission fragments emitted from adjacent pellets. These foil cassettes are shown in Figs. 4 and 5. The foil cassette was placed between two special PuO₂-UO₂ pellets, referred to as disk pellets, having flatter surfaces and the same composition as the regular pellets.

Fuel
Fuel pellet
Density
Diameter
Enrichment
Composition
²³⁵ U
²³⁸ U
²³⁸ Pu
²³⁹ Pu
²⁴⁰ Pu
²⁴¹ Pu
²⁴² Pu
O
Fuel pin
Cladding
Cladding
Cladding
Gap material

Here, (s) means, respectively, used as fuel, and UO₂ used

The discentered in the core. Cadmium was used to investigate the measurement by a 20-mm plugging device in Fig. 4. Cadmium, PuO₂-UO₂ fuel in a glove box at the Tokai V Fuel Development pin in which the normal (long), for the lower section of the upper section. Figure 6 shows the cut after irradiation to the cut. Plutonium was removed in the room where thereafter the foil

TABLE III
Specifications of Fuel

Fuel Type	0.54 wt% (s) ^a PuO ₂ -UO ₂	0.87 wt% (s) ^a PuO ₂ -UO ₂	0.87 wt% (r) ^a PuO ₂ -UO ₂	1.2 wt% UO ₂ ^b	1.5 wt% UO ₂ ^c
Fuel pellet					
Density, g/cm ³	10.17	10.17	10.25	10.36	10.38
Diameter, mm	14.69	14.72	14.68	14.80	14.77
Enrichment, wt%	0.542 $\left(\frac{\text{PuO}_2}{\text{PuO}_2 + \text{UO}_2} \right)$	0.862	0.874	1.203 (²³⁵ U)	1.499
Composition, wt%					
²³⁵ U	0.6214	0.6194	0.6194	1.057	1.317
²³⁸ U	86.782	86.503	86.493	86.793	86.563
²³⁸ Pu	0.000102	0.000145	0.00641		
²³⁹ Pu	0.4304	0.6849	0.4953		
²⁴⁰ Pu	0.04115	0.06584	0.1661		
²⁴¹ Pu	0.004359	0.00696	0.07217		
²⁴² Pu	0.000303	0.00051	0.02296		
O	12.12	12.12	12.13	12.15	12.12
Fuel pin					
Cladding material	Zircaloy-2			Al	
Cladding i.d., mm	15.06			15.03	
Cladding o.d., mm	16.68			16.73	
Gap material	Helium			Air	

^aHere, (s) and (r) designate standard-grade and reactor-grade plutonium containing ~91 and ~74% fissile plutonium, respectively.

^bUsed as the driver fuel.

^cUO₂ used in the previous experiments, Ref. 6.

The disk and adjacent pellets were carefully centered in the system axis by adhesive aluminum tape. Cadmium-covered foils were used to investigate epithermal neutrons. For subcadmium measurements, cadmium covering was provided by a 20-mm-wide, 200-mm-long ring and end-plugging disks (all 0.5 mm thick), located as shown in Fig. 4. The foil cassettes with or without cadmium disks were loaded together with the PuO₂-UO₂ pellets into the Zircaloy-2 cladding tube in a glove box of the Plutonium Fuel Division at the Tokai Works of the Power Reactor and Nuclear Fuel Development Corporation (PNC). The fuel pin in which the cassettes were loaded was half the normal length (i.e., the fuel was 100.0 cm long); for easier handling in the glove box. This lower section of the fuel pin was connected with the upper section before irradiation in the cluster. Figure 6 shows the pins.

After irradiation, the fuel pins were removed to the cutting glove box, shown in Fig. 7, in the Plutonium Handling Room located near the reactor room where the foil cassettes were recovered. Thereafter, the dysprosium foils were picked out of the foil cassettes in the next decontamination

glove box. The handling procedure necessary for obtaining uncontaminated irradiated foils is described in detail in a previous paper.¹⁵

For measurements in the coolant region, a 0.1-mm-thick sector foil was used as shown in the shaded section in Fig. 3 and in the close-up in Fig. 5. The sector foil, which was sandwiched in a 0.5-mm-thick acrylic acid resin holder, was irradiated. After irradiation, the sector foil was divided into seven pieces, from C-1 to C-7, as shown in Fig. 8, and each piece was counted for a time, depending on its activity and the counting efficiency.

The reaction rate distribution in the D₂O moderator was measured along the 0- and 45-deg directions by 7-mm-diam dysprosium foils. These foils were arranged in line on a 0.5-mm-thick aluminum holder, as shown in Fig. 9, which was suspended from the upper grid plate by a fine nylon thread. The holder was accurately and stably positioned between two calandria tubes by

¹⁵Y. NAKAMURA, Y. MIYAWAKI, N. SASAO, Y. HACHIYA, and A. SHIMAMURA, *J. Nucl. Sci. Technol.*, **9**, 277 (1972).

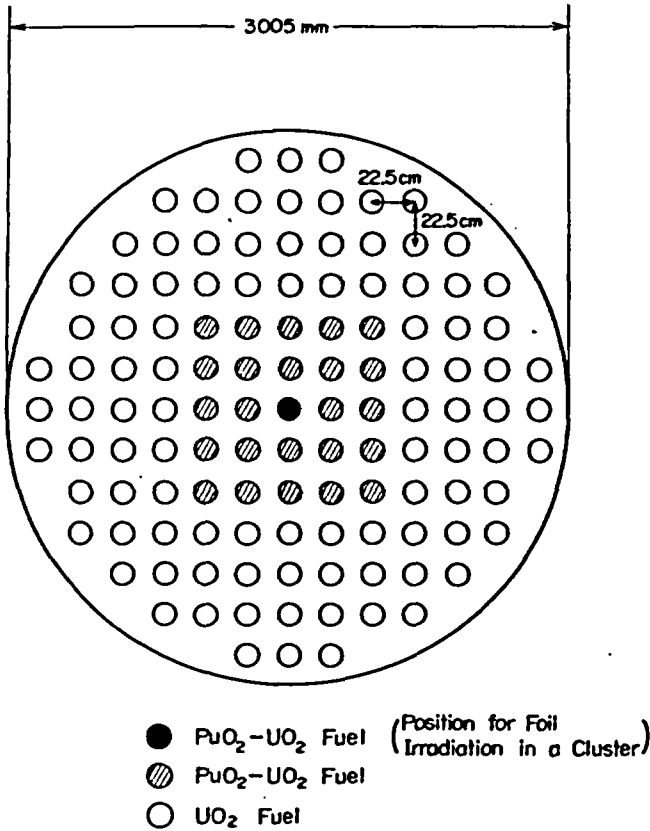


Fig. 2. Core configuration for 22.5-cm pitch lattice.

the two wings that protrude from its ends. Flux perturbation by the presence of this light-weight holder is thought to be negligible.

The dysprosium reaction rates at the surface of the pressure and calandria tubes were also measured with the same 7-mm-diam foils located at two identical positions around each surface, as shown in Fig. 3. The foil setting technique was as follows. A foil to be set on the inner surface of a tube was first fixed into a 0.1-mm-thick aluminum holder. Then, as shown in Fig. 9 (tool A), the holder was tied at both edges with a nylon thread and was tightly covered with adhesive tape of adequate cross section. This setup was then pressed by another tool, B, at the proper position in the calandria or pressure tube. Tool A is removed by cutting the nylon thread loop. The cross section of the adhesive tape was adjusted to raise the setup easily after irradiation by the upper portion of the nylon thread.

All the dysprosium foils except the cadmium-covered foils were located at the same vertical distance, 40 cm, from the lower grid plate, and were irradiated for 30 min at a power of 100 W [$\sim 10^8$ n/(cm²·s)]. After ~ 2 h of cooling time, the beta particles from ¹⁶⁵Dy (half-life = 139.9 min)

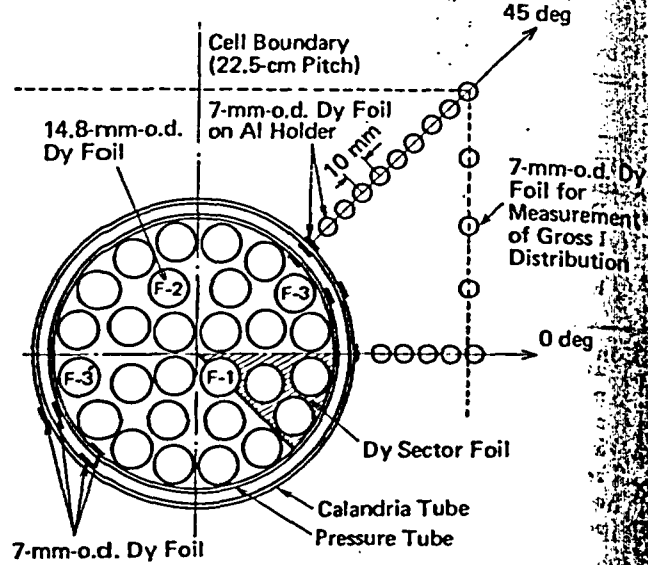


Fig. 3. Arrangement of dysprosium foils in central unit.

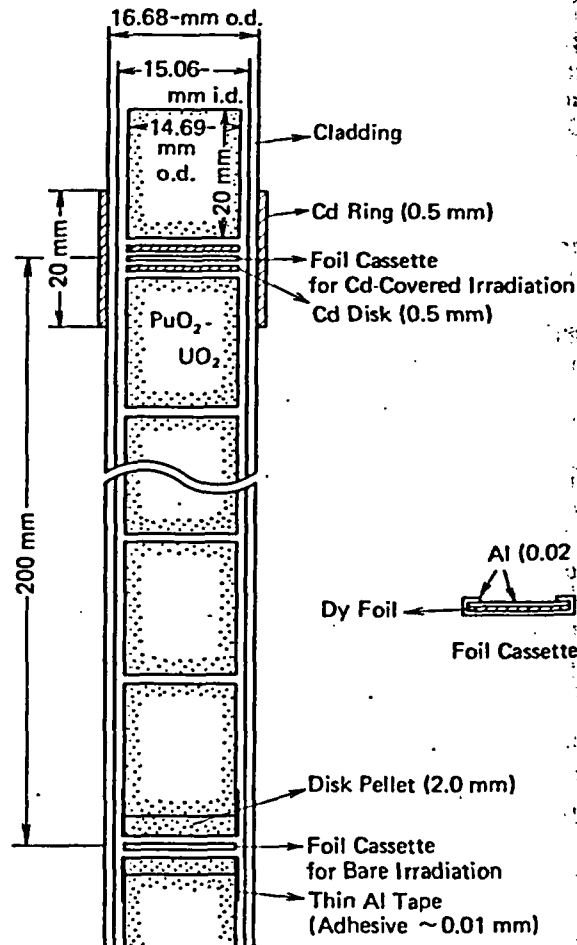


Fig. 4. Foil arrangement in PuO₂-UO₂ fuel pin.

Fig. 5. Foil and sector foils.



Fig. 7. Experiment.

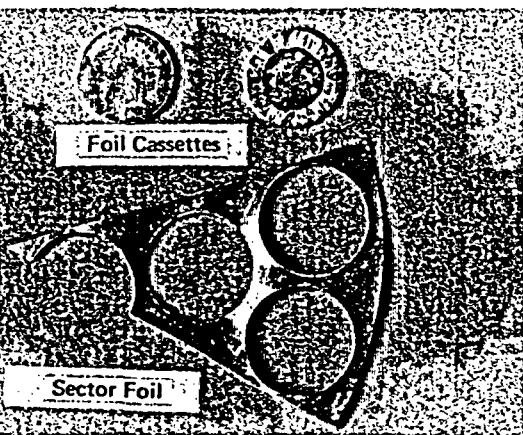


Fig. 5. Foil cassettes for measurement within plutonium fuel and sector foil for measurement in coolant.

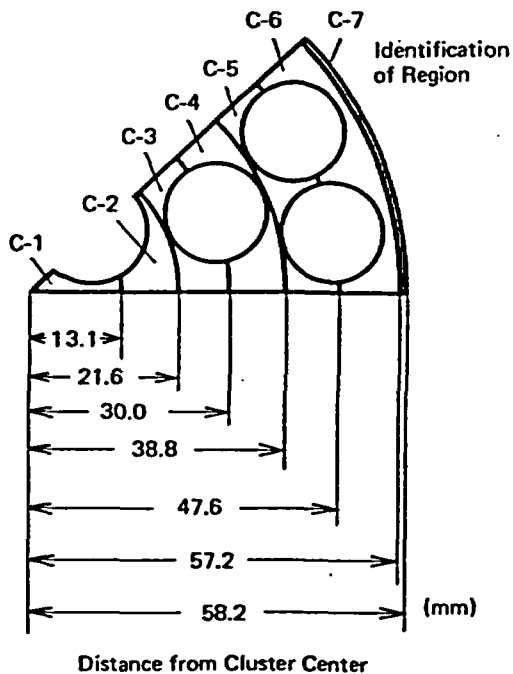


Fig. 8. Sector foil for measurement of the dysprosium reaction rate in the coolant region.

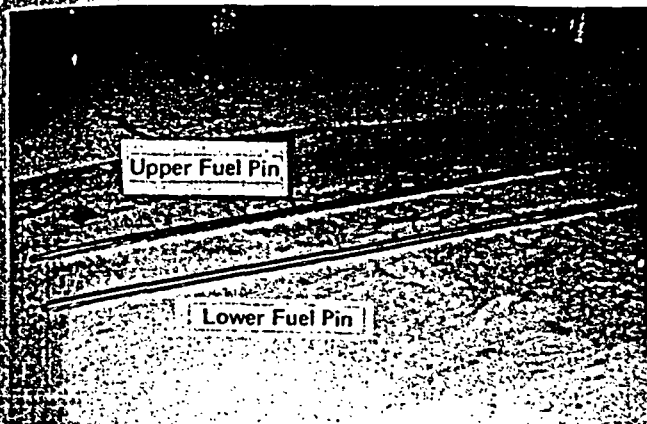


Fig. 6. Lower and upper plutonium fuel pins.

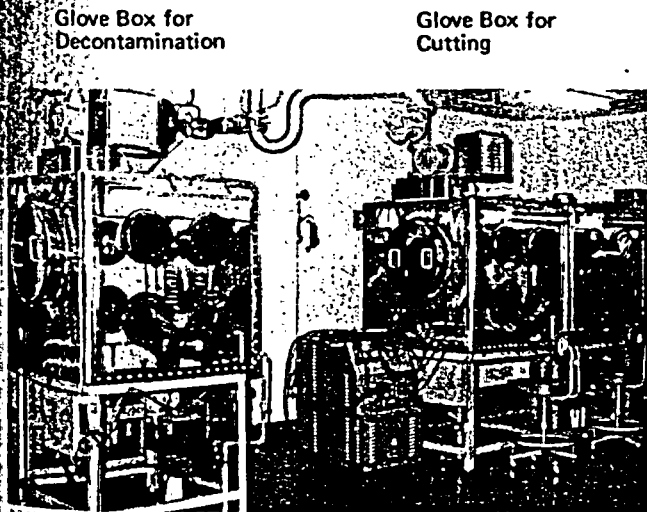


Fig. 7. Plutonium handling room in the heavy-water critical experiment section of PNC.

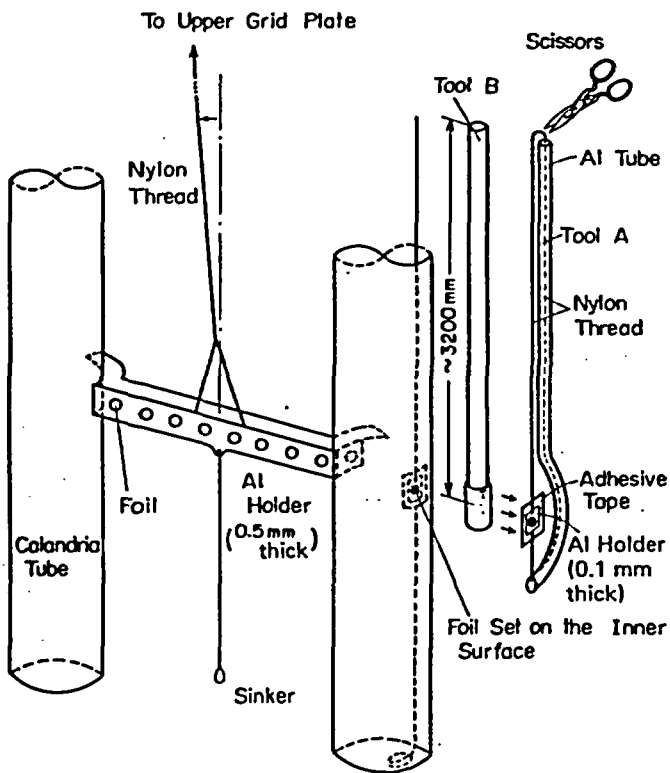


Fig. 9. Holder arrangement for measurement in the D₂O moderator and tools for locating foils on the inner surface of the calandria or pressure tubes.

were counted by an ordinary beta-particle counting system having a 2-in.-diam \times $\frac{1}{8}$ -in.-thick $\text{CaF}_2(\text{Eu})$ scintillator. Each foil was counted more than four times.

The reaction rate distribution was obtained from each set of counts by applying corrections for counting system background and dead time, the decay time, and the counting efficiency characteristic of the various foil shapes and weights. In addition to these corrections, the reaction rate distribution in the unit cell was corrected for the episcadmium reaction rate and also for the gross distribution, which was measured with the dysprosium foils placed at 2.25-cm intervals on an aluminum holder across the core diameter. The actual measured distribution, which is the mixture of gross and intracell distributions, is shown in Fig. 10 for the case of zero coolant void fraction in the 0.54-wt% $\text{PuO}_2\text{-UO}_2$ -fueled lattice. Six curves (A, B, C, D, E, and F) were obtained by the least-squares method using the reaction rates on periodically identical and symmetrical positions across the unit cells of the plutonium fuel region. These curves were normalized into one curve, and by using this resultant curve, the gross distribution was eliminated. Details of this experimental method are described in a separate report.¹⁶

After these corrections, the experimental error for the present dysprosium reaction rate distributions in the unit cell was estimated to be $\pm 2\%$, taking $\pm 1.0\%$ for the statistical error and $\pm 1.6\%$ for the systematic error. This systematic error includes errors of $\pm 0.6\%$ in counter dead time and counting efficiency, $\pm 0.6\%$ in the episcadmium activity correction factor, and $\pm 0.3\%$ in the correction for the gross distribution.

IV. RESULTS AND DISCUSSION

Figures 11 and 12 show the dysprosium reaction rate distributions in the unit cell for 0.54-wt% $\text{PuO}_2\text{-UO}_2$ fuel at 22.5- and 25.0-cm pitch lattices and zero void fraction. For the detailed comparison among various experimental distributions or between the experimental results and the calculation, some normalization should be made at an appropriate space point. In the present unit cell system, a point between the pressure and calandria tubes is thought to be proper for normalization, because the source and sink regions of thermal neutrons are clearly distinguished by the two tubes, especially at 100% void fraction. However, the detailed measurements around the surface of

¹⁶T. WAKABAYASHI, Y. HACHIYA, and N. FUKUMURA, "Measurement of Material Buckling in Cluster-Type Fuel Cores," ZN 941 74-82, Power Reactor and Nuclear Fuel Development Corporation (in Japanese) (1974).

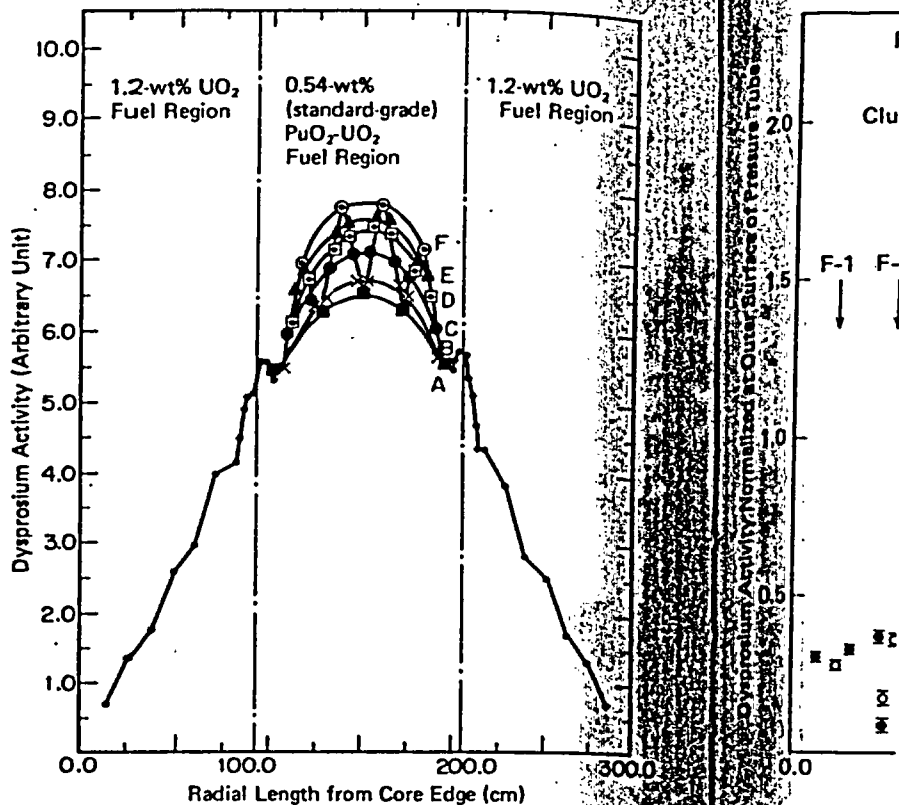


Fig. 10. Gross flux distribution for zero coolant void fraction in the 0.54-wt% standard-grade $\text{PuO}_2\text{-UO}_2$ fuel lattice.

the tubes have not been made in the earlier experiments^{3,6,7} due to the difficulty of setting foils in the correct positions on the inner surfaces of the long pressure and calandria tubes.

In the present experiment, the detailed distributions could be obtained by the foil-setting technique mentioned in the preceding section, resulting in an accurate normalization at the outer surface of the pressure tube. In addition to the problem of normalization, the thermal-neutron behavior around the boundary was made clear, as shown in the figures.

Results of the present systematic experiments led us to the following discussions of the dependence of thermal-neutron behavior on coolant void fraction, fuel enrichment, plutonium isotopic composition, and lattice pitch.

IV.A. Dependence on Coolant Void Fraction

The dependence of the thermal-neutron flux on the coolant void fraction is shown in Fig. 13 measured for the 0.54-wt% $\text{PuO}_2\text{-UO}_2$ fuel at the 22.5-cm lattice pitch.

The thermal-neutron flux depression in the fuel region is enhanced with increasing presence of

Fig. 11. Dysprosium reaction rate distribution in the unit cell for 0.54-wt% $\text{PuO}_2\text{-UO}_2$ fuel at 22.5-cm pitch and zero coolant void fraction.

the tubes have not been made in the earlier experiments^{3,6,7} due to the difficulty of setting foils in the correct positions on the inner surfaces of the long pressure and calandria tubes. In the present experiment, the detailed distributions could be obtained by the foil-setting technique mentioned in the preceding section, resulting in an accurate normalization at the outer surface of the pressure tube. In addition to the problem of normalization, the thermal-neutron behavior around the boundary was made clear, as shown in the figures. Results of the present systematic experiments led us to the following discussions of the dependence of thermal-neutron behavior on coolant void fraction, fuel enrichment, plutonium isotopic composition, and lattice pitch. IV.A. Dependence on Coolant Void Fraction The dependence of the thermal-neutron flux on the coolant void fraction is shown in Fig. 13 measured for the 0.54-wt% $\text{PuO}_2\text{-UO}_2$ fuel at the 22.5-cm lattice pitch. The thermal-neutron flux depression in the fuel region is enhanced with increasing presence of

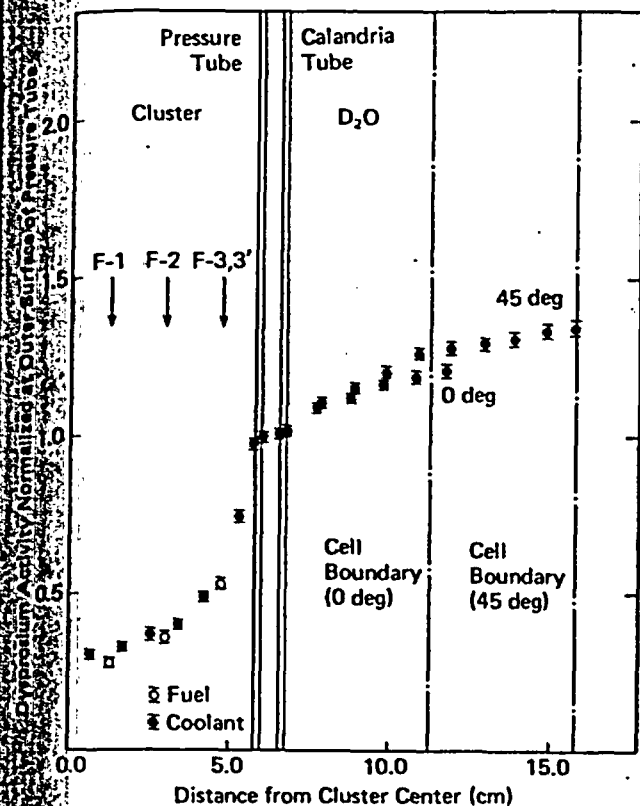


Fig. 11. Dysprosium reaction rate distribution for zero coolant void fraction in 0.54-wt% standard-grade $\text{PuO}_2\text{-UO}_2$ fuel in a 22.5-cm pitch lattice.

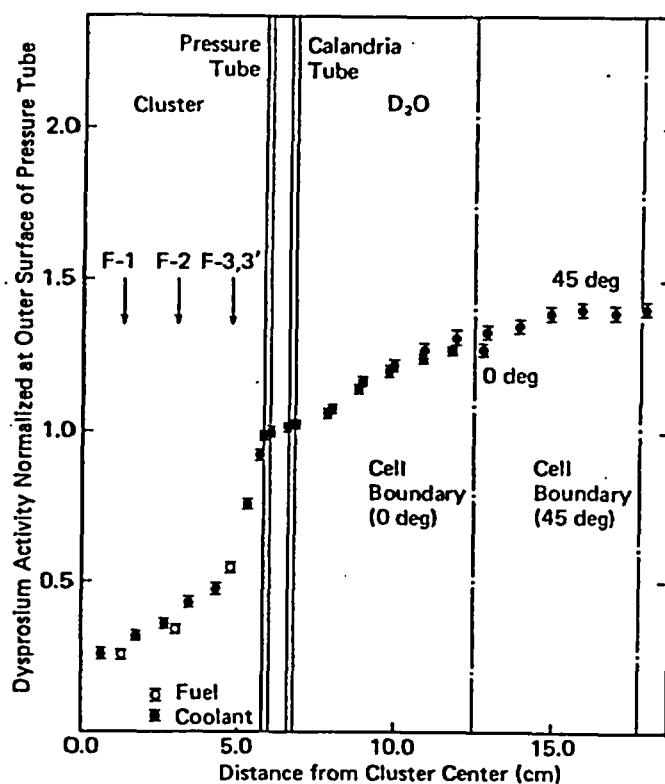


Fig. 12. Dysprosium reaction rate distribution for zero coolant void fraction in 0.54-wt% standard-grade $\text{PuO}_2\text{-UO}_2$ fuel at a 25.0-cm pitch lattice.

H_2O coolant (i.e., decreasing coolant void fraction). However, with increasing presence of H_2O coolant, the thermal-neutron flux distribution is seen to be flattened in the D_2O region. These tendencies have also been observed in the previous experiment⁶ with UO_2 fuel lattices. The former tendency can be considered due to a shortening of the average diffusion length in the fuel region by the presence of the H_2O coolant; the H_2O coolant enhances the thermal-neutron self-shielding effect in the fuel region, and the latter is due to the enhanced reflection by the H_2O coolant of the thermal neutrons emanating from the D_2O moderator region.

In a quantitative discussion about the tendency in the fuel region, the average diffusion length was calculated using the group constants obtained by transport theory¹⁴ and listed in Table IV.

The values for 0, 30, and 70% void fractions cluster in groups far removed from the value for 100%, as seen in Fig. 13. These subtle differences in the coolant-filled lattices and the large departure at 100% void fraction can be systematically comprehended in terms of the average diffusion length. These tendencies are also discussed in Sec. IV.E.

IV.B. Dependence on Fuel Enrichment

The dysprosium reaction rate distributions of the 0.54-wt% and 0.87-wt% standard-grade and 0.87-wt% reactor-grade enriched $\text{PuO}_2\text{-UO}_2$ fuels measured in the 22.5-cm pitch lattice are shown in Fig. 14. It is seen that increasing standard-grade fuel enrichment (0.54 wt% \rightarrow 0.87 wt%) tends to accentuate the depression of the thermal-neutron flux within the fuel region, as well as the corresponding rise in the D_2O moderator. The tendency of the distribution in the D_2O moderator region is the opposite of the tendency with increasing H_2O coolant.

The accentuated depression can be ascribed to enhancement of the thermal-neutron self-shielding effect due to absorption in the fuel and the corresponding tendency in the moderator region to increased thermal-neutron current flowing from the D_2O toward the fuel region.

As seen further in Fig. 14, the variation of the thermal-neutron flux in the fuel region in the case of 100% void fraction is larger than that with zero void fraction with the same fuel enrichment. This tendency can be explained by the fact that the variation in the average diffusion length shown in Table IV is larger with 100% void fraction than

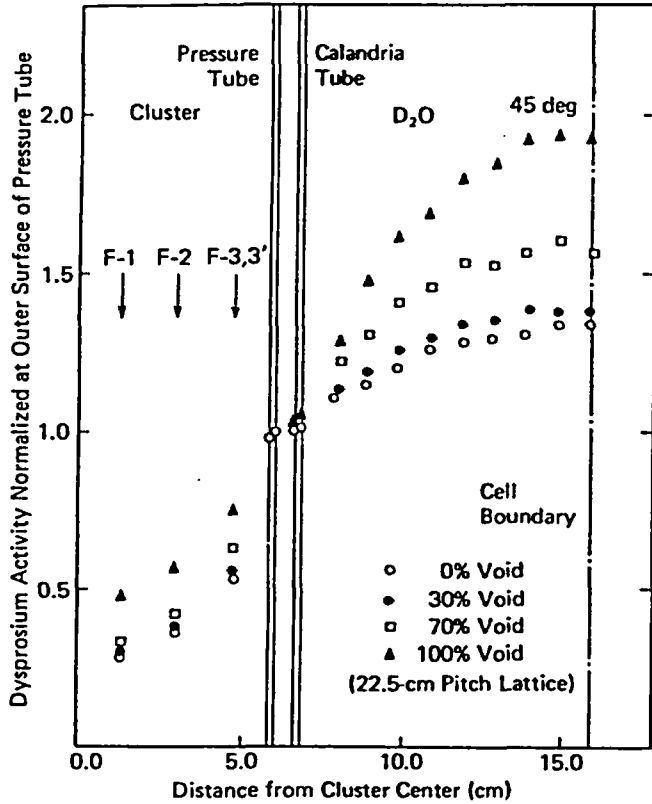


Fig. 13. Dependence of thermal-neutron flux distributions on the coolant void fraction in a 0.54-wt% standard-grade $\text{PuO}_2\text{-UO}_2$ fuel lattice.

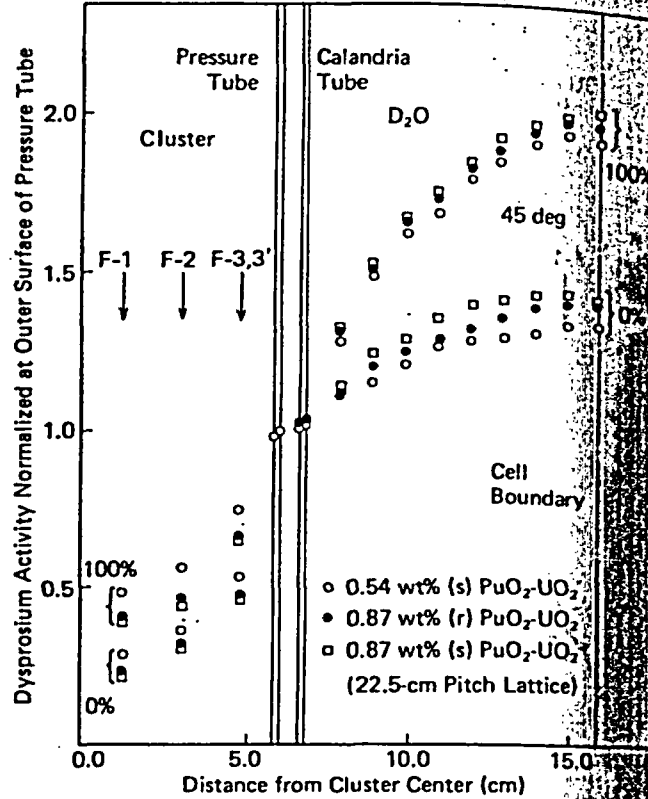


Fig. 14. Dependence of thermal-neutron flux distributions on the fuel enrichment and plutonium isotopic composition.

Group Cc	Lattice Pitch
	22.5 cm
	25.0 cm

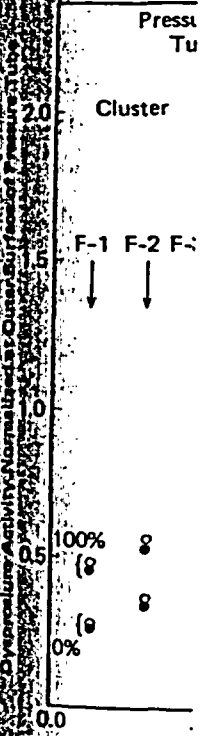


Fig. 15. Dependence on the lattice pitch of thermal-neutron flux distributions in a 0.54-wt% $\text{PuO}_2\text{-UO}_2$ fuel.

that with zero void fraction. The reason is that the change in the absorption cross section of the fuel region, predominantly in the value of $\Sigma_{tr}\{L^2 = \frac{1}{3}[1/(\Sigma_a \Sigma_{tr})]\}$, is weakened by the presence of a large transport cross section of the H_2O coolant.

IV.C. Dependence on Plutonium Isotopic Composition

As also seen in Fig. 14, the depression of the thermal-neutron flux in the fuel region for reactor-grade 0.87-wt% $\text{PuO}_2\text{-UO}_2$ fuel is smaller than that of standard-grade 0.87-wt% $\text{PuO}_2\text{-UO}_2$ fuel. In the D_2O region, the flux distribution is more flattened.

This tendency is easily explained by the fact that the reactor-grade fuel corresponds to a lower fuel enrichment than that of the standard-grade fuel because either the 2200 m/s macroscopic absorption cross section summed over all the isotopes or the thermal macroscopic absorption cross section, including resonance absorption peaks calculated by the LAMP-DCA (listed in Table IV), is smaller in the case of the reactor-grade 0.87-wt%-enriched $\text{PuO}_2\text{-UO}_2$ fuel.

IV.D. Dependence on Lattice Pitch

The depression of the thermal-neutron flux in the fuel region of the 25.0-cm-pitch lattice is appreciably larger than that of 22.5-cm pitch, as seen in Fig. 15. It is considered that this tendency originates in the increase in neutron absorption in the fuel by softening of the thermal-neutron spectrum due to an increase in the region of the D_2O moderator. The absorption cross section in the LAMP-DCA calculations, Table IV, also indicates a softer neutron spectrum in the larger 25.0-cm pitch lattice.

In the D_2O moderator, when the lattice pitch is extended from 22.5 to 25.0 cm, the thermal-neutron flux distributions apparently become higher at the cell boundary, as seen in Fig. 15. This tendency is accounted for by the increase of the slowing down effect in the D_2O moderator region.

IV.E. Thermal Disadvantage Factors

Here, the thermal disadvantage factor is defined as the average dysprosium reaction rate in the fine distribution in each region: coolant, pressure tube, calandria tube, and D_2O moderator, divided

by the dysprosium reaction rate in the fuel pins. The reaction rate was fitted to a square-law distribution in the moderator region.

TABLE IV

Group Constants and Diffusion Length for Various Fuel Lattices Calculated by the LAMP-DCA Code

Lattice Pitch	Fuel Enrichment	Void Fraction (%)	Σ_a (cm ⁻¹)	Σ_{tr} (cm ⁻¹)	$L^2 = \frac{1}{3\Sigma_a\Sigma_{tr}}$ (cm ²)	L (cm)
22.5 cm	0.54 wt% (s) PuO ₂ -UO ₂	0	0.103	1.255	2.579	1.606
		30	0.101	0.976	3.381	1.839
		70	0.096	0.608	5.711	2.390
		100	0.088	0.303	12.419	3.524
	0.87 wt% (r) PuO ₂ -UO ₂	0	0.121	1.257	2.192	1.481
		100	0.105	0.322	9.859	3.140
0.87 wt% (s) PuO ₂ -UO ₂	0	0.127	1.257	2.088	1.445	
	100	0.109	0.326	9.381	3.063	
25.0 cm	0.54 wt% (s) PuO ₂ -UO ₂	0	0.107	1.260	2.472	1.572
		100	0.092	0.307	11.802	3.435

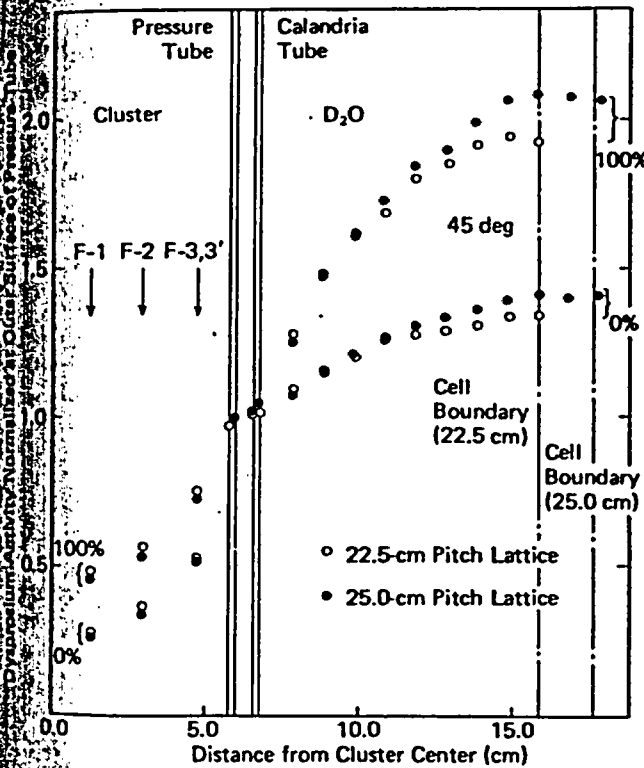


Fig. 15. Dependence of thermal-neutron flux distributions on the lattice pitch measured with 0.54-wt% standard-grade PuO₂-UO₂ fuel.

by the dysprosium reaction rate averaged in all the fuel pins.

The reaction rate distribution in the coolant was fitted to the parabolic curve by the least-squares method. For distribution in the D₂O moderator region, a smooth spherical curve having

variables r (distance from cluster center) and θ (angle from 0 deg) was determined by fitting it by the least-squares method to the measured values along the four peripheries: along the two directions 0 and 45 deg, on the outer surface of the calandria tube, and at the cell boundary, as shown in Fig. 3.

The thermal disadvantage factors in each region are shown in Tables V and VI. As seen in these tables, the thermal disadvantage factor in each region increases with an increase in H₂O coolant, fuel enrichment, and lattice pitch. However, in the case of coolant void fraction, the maximum value in the D₂O region is seen at 30% in both lattice pitches.

For the comprehension of this discrepancy, the thermal disadvantage factors measured for the standard-grade 0.54-wt% PuO₂-UO₂ fuel in the 22.5-cm pitch lattice were separated into numerator and denominator (average reaction rate in the fuel and in the D₂O moderator region), and they are shown in Fig. 16 with normalization at zero void fraction.

As mentioned in Sec. IV.A, the main effect of the H₂O coolant on the fuel region is understood as the enhancement of self-shielding, and on the D₂O moderator region, the reflection of the thermal neutrons back to the D₂O moderator. As seen in Fig. 16, the enhancement of the self-shielding effect is almost saturated at around 30% void fraction with the increasing presence of H₂O coolant. This means that introduction of more than 70% H₂O into the coolant mixture (<30% void fraction) has only a small effect on accentuating the depression in the fuel region. However, as also seen in the figure, the thermal-neutron reflection effect that makes the thermal-neutron

TABLE V
Thermal Disadvantage Factor for the 22.5-cm Pitch Lattice

Region	Fuel							
	0.54 wt% (s) PuO ₂ -UO ₂				0.87 wt% (s) PuO ₂ -UO ₂		0.87 wt% (r) PuO ₂ -UO ₂	
	Coolant Void Fraction (%)							
	0	30	70	100	0	100	0	100
Coolant								
Experiment	1.245 ± 0.051	1.326 ± 0.053	1.243 ± 0.052	---	1.359 ± 0.054	1.194 ± 0.048	1.343 ± 0.054	1.149 ± 0.046
METH ^a	1.292	1.267	1.219	1.059	1.408	1.077	1.352	1.070
LAMP ^a	1.291	1.333	1.272	1.142	1.387	1.228	1.365	1.211
Pressure tube								
Experiment	2.217 ± 0.078	2.146 ± 0.075	1.883 ± 0.066	1.504 ± 0.053	2.564 ± 0.091	1.795 ± 0.063	2.469 ± 0.086	1.754 ± 0.061
METH	2.232	2.105	1.873	1.481	2.519	1.637	2.445	1.590
LAMP	2.252	2.208	1.901	1.548	2.545	1.855	2.433	1.786
Calandria tube								
Experiment	2.266 ± 0.079	2.227 ± 0.079	1.970 ± 0.069	1.570 ± 0.055	2.672 ± 0.094	1.876 ± 0.066	2.546 ± 0.089	1.825 ± 0.064
METH	2.254	2.128	1.906	1.526	2.544	1.689	2.469	1.641
LAMP	2.309	2.274	1.975	1.641	2.616	1.978	2.499	1.900
Moderator								
Experiment	2.670 ± 0.081	2.685 ± 0.082	2.557 ± 0.076	2.335 ± 0.070	3.251 ± 0.113	2.865 ± 0.086	3.032 ± 0.111	2.767 ± 0.097
METH	2.699	2.625	2.517	2.271	3.101	2.638	2.978	2.510
LAMP	2.736	2.764	2.527	2.311	3.142	2.846	2.966	2.695

^aCalculated values by the METHUSELAH-II and LAMP-DCA codes.

In Fig. 17

resonance. s the
and plutonium
of the present
at 1.1 eV for 3rd
large resonan
tion to this
to be approxi
of uranium ab
in the low

V. COM

maximum val
range factor

distribution b

reases with

coolant. As

Calculated v

LAMP

METH

Experiment

Moderator

LAMP

METH

Experiment

Calandria tub

LAMP

METH

Experiment

Calandria tub

LAMP

METH

Experiment

Pressure tub

LAMP^a

METH^a

Experiment

Coolant

Region

TABLE VI
Thermal Disadvantage Factor for the 25.0-cm Pitch Lattice

Region	Fuel				
	0.54 wt% (s) PuO ₂ -UO ₂			0.87 wt% (r) PuO ₂ -UO ₂	
	Coolant Void Fraction (%)				
	0	30	100	0	100
Coolant					
Experiment	1.272 ± 0.053	1.249 ± 0.049	1.146 ± 0.043	1.361 ± 0.054	1.168 ± 0.05
METH ^a	1.294	1.265	1.058	1.349	1.071
LAMP ^a	1.300	1.279	1.143	1.350	1.191
Pressure tube					
Experiment	2.273 ± 0.072	2.208 ± 0.075	1.572 ± 0.055	2.597 ± 0.091	1.773 ± 0.063
METH	2.331	2.174	1.488	2.564	1.620
LAMP	2.262	2.193	1.550	2.481	1.776
Calandria tube					
Experiment	2.332 ± 0.073	2.276 ± 0.082	1.653 ± 0.062	2.694 ± 0.092	1.894 ± 0.066
METH	2.354	2.200	1.533	2.592	1.683
LAMP	2.325	2.262	1.643	2.556	1.890
Moderator					
Experiment	2.832 ± 0.071	2.916 ± 0.081	2.610 ± 0.095	3.374 ± 0.115	3.055 ± 0.111
METH	2.925	2.822	2.421	3.269	2.693
LAMP	2.880	2.874	2.520	3.206	2.980

^a Calculated value by the METHUSELAH-II and LAMP-DCA codes.

distribution in the D₂O region flatten, still increases with the increasing presence of the H₂O coolant. As a result, it is understood that the maximum value of the thermal-neutron disadvantage factor is present at ~30% void fraction.

V. COMPARISON WITH THE RESULTS FROM UO₂ FUEL

In the low neutron energy region, the structure of uranium absorption cross section is considered to be approximately of the $1/v$ law type. In addition to this $1/v$ part, however, plutonium has a large resonance at 0.3 eV for ²³⁹Pu and ²⁴¹Pu and at 1 eV for ²⁴⁰Pu. If the dysprosium reaction rate of the present PuO₂-UO₂ fuel is plotted as a function of the $1/v$ part that is common to the uranium and plutonium, the difference in the observed tendencies should exhibit the effect caused by the resonance.

In Fig. 17, the average dysprosium reaction

rates in the fuel are shown as a function of the 2200 m/s macroscopic absorption cross section with normalization at the pressure tube. They represent 1.2- and 1.5-wt% ²³⁵U-enriched UO₂ fuel and standard-grade 0.54-wt% and 0.87-wt%, and reactor-grade 0.87-wt% PuO₂-UO₂ fuels of 0 and 100% coolant void fraction.

Through the comparison of these results, the following facts are summarized:

1. Changes in the average reaction rate in the fuel with increase in fuel enrichment are larger for plutonium than for uranium.
2. Change in the average reaction rate in the fuel is larger with 100% void fraction than with zero in cases for both uranium and plutonium.

The larger gradient in the reaction rate in plutonium fuels than that of the $1/v$ part (uranium fuel) is believed to be entirely caused by the

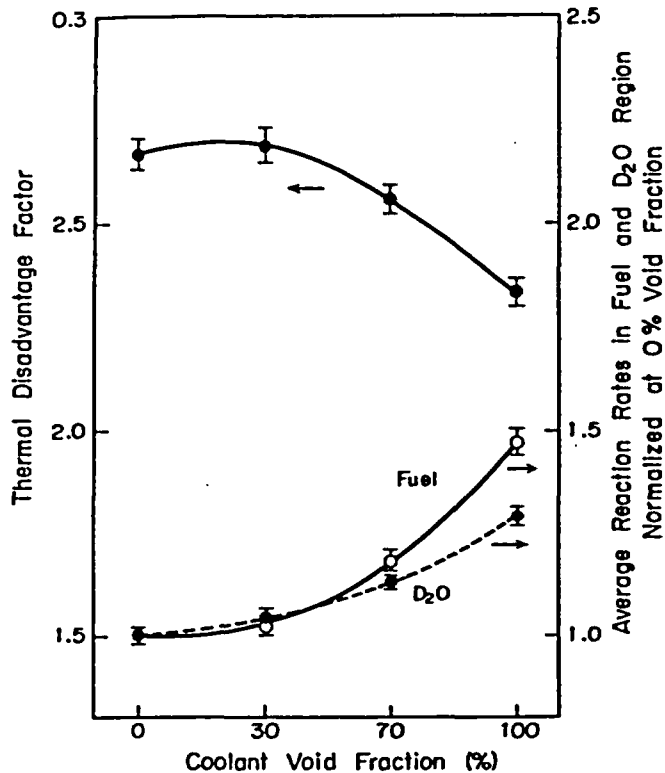


Fig. 16. Dependences of the thermal disadvantage factor and average reaction rates in the fuel and D₂O regions on coolant void fraction.

enhanced thermal-neutron absorption by the resonances. At zero void fraction, the average diffusion length is thought to be largely affected by the presence of the H₂O coolant, as discussed in Sec. IV.B, resulting in a weakened change of fuel itself, such as an increase in enrichment or an increase in the resonance part. The experimental results (the fact that at zero void fraction the variation of the average reaction rate is smaller in both uranium and plutonium fuels, including the reactor-grade fuel) are understood by this effect of the H₂O coolant.

VI. COMPARISON WITH CALCULATION

The present experimental results are compared with two calculation codes: the METHUSELAH-II code^{11,12} and the LAMP-DCA code system.^{13,14} The METHUSELAH-II code developed by Alpiar¹¹ has been used for survey calculation to serve in the nuclear design of FUGEN.

For the purpose of obtaining better calculational accuracy, the LAMP-DCA code system has been developed by the Japan Atomic Energy Research Institute¹³ and by PNC (Ref. 14). It is a set of programs solving the integral neutron transport

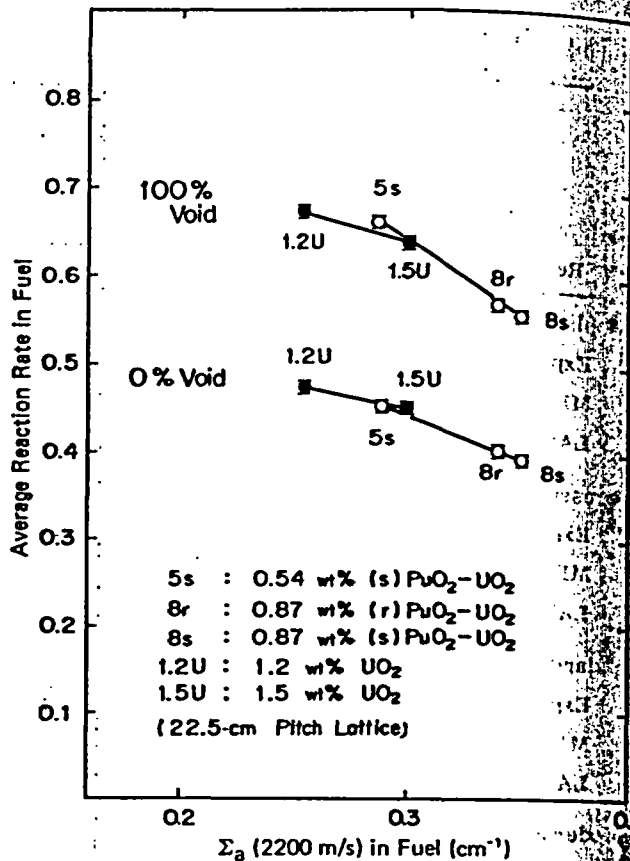


Fig. 17. Average reaction rate in fuel as a function of the 2200 m/s macroscopic absorption cross section.

equation of a reactor cell, with a cylindrical outer boundary, by the method of collision probability. For the cell geometry, it does not use any approximation such as the subcell model of the fuel region adopted in the METHUSELAH-II code. This code system is divided into three groups of programs for the thermal, resonance, and fast energy neutrons. For the thermal energy of the present problems, the LAMP-DCA comprises four programs: PIXSE, CLUP, PIJF, and FLUX. Microscopic cross sections of 50 energy groups are mainly from ENDF/B-III. In PIXSE, the macroscopic cross sections, including the scattering matrix, are processed. The collision probability P_{ij} is calculated by the CLUP program. The space- and energy-dependent flux distribution is solved by the PIJF program and is used to calculate region-averaged cross sections in single- or multigroup structures. In the FLUX program, the activation distribution and its thermal disadvantage factor are calculated for various nuclides.

Calculated results relevant to the thermal disadvantage factor are presented in Tables V and VI. The results of the METHUSELAH-II

calculations are within 5% of the corresponding to 0, lattices without calculated values standard-grade pitch lattice, and discrepancy is more than 10%. On the other hand, the LAMP-DCA results are in good agreement with the reactor-grade fuel results, being within 5% of the corresponding to 0, lattice pitch.

Thermal-neutron resonance absorption has been made clear by the present experiments. The results are in good agreement with the reactor-grade fuel results, being within 5% of the corresponding to 0, lattice pitch.

With an increase in the thermal disadvantage factor, the thermal disadvantage factor is calculated around the boundary of the moderator. The thermal disadvantage factor is calculated around the boundary of the moderator.

Calculations agree with the experimental results to within 5% for the coolant-filled lattices corresponding to 0, 30, and 70% void fraction. In the lattices without coolant (100% void fraction), calculated values agree within 5% only in the case of standard-grade 0.54-wt% PuO₂-UO₂ fuel of 22.5-cm pitch lattice, while, in the other cases, the discrepancy is more than 5%.

On the other hand, the results calculated by LAMP-DCA are, irrespective of the presence of coolant, in good agreement with the experimental results, being within 5% for changes in fuel enrichment, plutonium isotopic composition, and lattice pitch.

VII. CONCLUSION

Thermal-neutron behavior in a highly heterogeneous cluster-type plutonium fuel lattice has been made clear by the measurement of dysprosium reaction rate distributions covering three different plutonium fuels, four coolant void fractions, and two lattice pitches and by comparison with the results of previously obtained UO₂-fueled experiments. Especially with the use of the foil-locating technique applicable to the inside surface of long calandria and pressure tubes, developed in the present experiment, the neutron behavior around the boundary between the fuel region and the moderator region was clarified.

With an increase in H₂O coolant, the depression of the thermal-neutron flux, caused by enhancement of the self-shielding effect, is almost saturated at around 30% void fraction. On the other hand, the thermal-neutron reflection effect, which

flattens the thermal-neutron flux distribution in the D₂O region, still increases with an increase in the H₂O coolant. From these tendencies, the increase in the thermal disadvantage factor in the D₂O region to a maximum at around 30% void fraction is explained.

The depression of the thermal-neutron flux in the fuel region is larger in the plutonium fuel lattice than in the uranium fuel lattice because the thermal-neutron absorption in the plutonium fuel is enhanced by the resonances in addition to the larger $1/\nu$ cross section of plutonium than that of uranium. This property of the plutonium fuel appears markedly at 100% void fraction, but less at zero void fraction because this property is weakened by the presence of the H₂O coolant.

Calculations by the LAMP-DCA code are in good agreement with the experimental results, being within 5% in the case of changes in coolant void fraction, fuel enrichment, plutonium isotopic composition, and lattice pitch.

ACKNOWLEDGMENTS

The authors are much indebted to K. Iijima, who made preliminary measurements of the present experiments and gave helpful advice thereafter. We are also grateful to N. Fukumura, A. Nishi, and I. Minatsuki for their help with the experiments and for fruitful discussions.

We wish to thank Y. Miyawaki, H. Sakata, and the staff members of the Heavy Water Critical Experiment Section, Oarai, PNC, and particularly K. Higuchi for their support in this series of experiments.

For the fabrication of the experimental plutonium fuel pins, the authors are grateful to the members of the Plutonium Fuel Division at the Tokai Works of PNC. Acknowledgment is further due to H. Kadotani (Century Research Center) for his help on the LAMP-DCA code calculation.